

OPEN

# 17 $\alpha$ Estradiol promotes plasticity of spared inputs in the adult amblyopic visual cortex

Deepali C. Sengupta<sup>1</sup>, Crystal L. Lantz<sup>2</sup>, M. A. Karim Rumi<sup>3,4</sup> & Elizabeth M. Quinlan<sup>1,2\*</sup>

The promotion of structural and functional plasticity by estrogens is a promising approach to enhance central nervous system function in the aged. However, how the sensitivity to estrogens is regulated across brain regions, age and experience is poorly understood. To ask if estradiol treatment impacts structural and functional plasticity in sensory cortices, we examined the acute effect of 17 $\alpha$ -Estradiol in adult Long Evans rats following chronic monocular deprivation, a manipulation that reduces the strength and selectivity of deprived eye vision. Chronic monocular deprivation decreased thalamic input from the deprived eye to the binocular visual cortex and accelerated short-term depression of the deprived eye pathway, but did not change the density of excitatory synapses in primary visual cortex. Importantly, we found that the classical estrogen receptors ER $\alpha$  and ER $\beta$  were robustly expressed in the adult visual cortex, and that a single dose of 17 $\alpha$ -Estradiol reduced the expression of the calcium-binding protein parvalbumin, decreased the integrity of the extracellular matrix and increased the size of excitatory postsynaptic densities. Furthermore, 17 $\alpha$ -Estradiol enhanced experience-dependent plasticity in the amblyopic visual cortex, by promoting response potentiation of the pathway served by the non-deprived eye. The promotion of plasticity at synapses serving the non-deprived eye may reflect selectivity for synapses with an initially low probability of neurotransmitter release, and may inform strategies to remap spared inputs around a scotoma or a cortical infarct.

Age-related constraints in synaptic plasticity have long been associated with a decrease in circulating sex hormones. Accordingly, estrogen therapy (estradiol valerate) is reported to prevent age-related cognitive impairment and improve verbal memory in oophorectomized premenopausal women<sup>1</sup>. Similar estrogen therapy reduces the development of all-cause dementia if initiated by age 65. The benefits of estrogens have also been demonstrated in animal models. In aged rhesus macaques, estrogen replacement (estradiol cypionate) following ovariectomy (OVX) reverses age-related cognitive impairment<sup>2</sup>. In OVX rats, treatment with 17 $\alpha$ -estradiol ( $\alpha$ E2), a stereoisomer of the main circulating estradiol (E2), improved object/place recognition and enhanced spatial working memory<sup>3</sup>. E2 treatment also improved water maze memory retrieval and reduced the severity score after traumatic brain injury in adult OVX mice (11–13 months<sup>4</sup>). The majority of these investigations utilized gonadectomized subjects to control for circulating hormone levels, and estrogen treatment in intact subjects produces more modest effects<sup>5,6</sup>. Importantly, gonadally-intact non-human primates experience less multi-synaptic bouton loss in the prefrontal cortex with age than OVX cohorts<sup>7</sup>, suggesting more severe neurological consequences with surgically induced menopause than natural aging.

Circulating estrogens are proposed to play a permissive role in activity-dependent synaptic plasticity by promoting the maintenance of synapse number and neuronal excitability. Consequently, the age-related decrease in circulating E2 correlates with a decrease in synaptic glutamate receptor density, and inhibition of E2 biosynthesis induces acute spine synapse loss<sup>8,9</sup>. Similarly, dendritic spine density and the magnitude of long term potentiation in the hippocampus and cortex are increased by E2 in intact and OVX adult rats<sup>10–12</sup>. Importantly, E2 delivery to intact male or intact and OVX female rats increases paired pulse depression, enhances synaptic strength, and promotes activity-dependent synaptic potentiation at excitatory synapses<sup>13–15</sup>.

<sup>1</sup>Neuroscience and Cognitive Science Program, University of Maryland, College Park, MD, 20742, United States.

<sup>2</sup>Department of Biology, University of Maryland, College Park, MD, 20742, United States. <sup>3</sup>Department of Pathology and Laboratory Medicine, University of Kansas Medical Center, Kansas City, KS, 66160, United States. <sup>4</sup>Institute for Reproduction and Perinatal Research, University of Kansas Medical Center, Kansas City, KS, 66160, United States.

\*email: [equinlan@umd.edu](mailto:equinlan@umd.edu)

The impact of estrogens on central nervous system function has been elucidated primarily in hippocampus and prefrontal cortex, areas known to express estrogen receptors (ERs) in young (3–4 months), middle-aged (9–11 months), and aged (19–24 months) female rats<sup>16–18</sup>. Classical estrogen signaling is mediated by cytoplasmic receptors that translocate to the nucleus to bind DNA and regulate transcription. However, E2 also enhances cognition and plasticity independently of transcription<sup>19,20</sup>. ERs associated with the plasma membrane and/or cytoplasmic organelles likely mediate the non-transcriptional regulation of synaptic function<sup>21,22</sup>. The canonical estrogen receptors, estrogen receptor  $\alpha$  (ER $\alpha$ ) and estrogen receptor  $\beta$  (ER $\beta$ ) are present at multiple sites in neurons<sup>16,23,24</sup>. ER $\alpha$  is observed in nuclei, cytoplasm and the presynaptic compartment of pyramidal neurons in hippocampal CA1, and immunogold electron microscopy (EM) localizes ER $\alpha$  to dendritic spines<sup>25</sup>. Immunogold EM also localizes ER $\beta$  to pre- and postsynaptic compartments of asymmetric synapses in CA1 in female rats, which persist following OVX and are increased by E2 treatment<sup>17</sup>. ER $\alpha$  and ER $\beta$  puncta co-localize with the postsynaptic scaffold protein PSD95, and E2 delivery recruits PSD95 to synapses in cultured neurons<sup>26</sup>. ER $\alpha$  is also present in approximately one-third of the inhibitory boutons that innervate pyramidal neuron somata in hippocampal CA1<sup>27</sup>. Presynaptic ER $\alpha$  co-localizes with cholecystokinin, is associated with clusters of synaptic vesicles and is mobilized toward the synapse by E2. Importantly, expression of membrane ERs persists in the adult hippocampus and prefrontal cortex following OVX<sup>16–18</sup>. In contrast, there is little consensus on the distribution or role of ERs in primary sensory cortices of adults, due in part to conflicts between previous reports, which also differ in age, species, sex and gonadal state<sup>28–32</sup>.

Here we examine the distribution of estrogen receptors in the primary visual cortex (V1) of adult male and female Long Evans (LE) rats following chronic monocular deprivation (cMD). cMD initiated at eye opening mimics the presence of a unilateral congenital cataract from birth and induces severe amblyopia that is highly resistant to reversal in adulthood<sup>33,34</sup>. Importantly, in the binocular region of the amblyopic visual cortex (V1b), synapses serving the deprived eye are weak, sparse and untuned, while synapses serving the non-deprived eye retain normal strength, density and stimulus selectivity<sup>35</sup>. In addition, the reduction in synaptic density and cortical function induced by cMD mimics changes observed during normal aging or in response to ischemic damage. We asked if acute treatment with estradiol can enhance plasticity in V1 of adult amblyopic rodents. We find that a single low dose of  $\alpha$ E2, which induces ~2 fold greater synaptogenesis in the hippocampus than an equivalent dose of E2<sup>36,37</sup> reduced the expression of the calcium binding protein parvalbumin (PV), reduced the integrity of the extracellular matrix, and increased the expression of PSD95. Furthermore,  $\alpha$ E2 treatment enhanced experience-dependent plasticity in the amblyopic cortex and promoted stimulus-selective response potentiation selectively in the pathway served by the non-deprived eye.

## Materials and Methods

**Subjects.** Long Evans (LE) Rats (strain 006, RRID:RGD\_2308852) were purchased from Charles River Laboratories (Raleigh, NC). Equal numbers of adult (>postnatal day 180, >P180) males and females were used. Animals were raised in 12/12 hour light/dark cycle and experiments were performed, or subjects were sacrificed, 6 hours into the light phase. Brains from 8–12 week old female ER $\beta$ <sup>-/-</sup> rats were provided by M.A. Karim Rumi of the University of Kansas Medical Center<sup>38</sup>. All procedures were approved by the University of Maryland Institutional Animal Care and Use Committee and were carried out in accordance with the Guide for the Care and Use of Laboratory Animals.

**Monocular deprivation.** P14 LE rat pups were anesthetized with ketamine/xylazine (100 mg/10 mg/kg, intraperitoneal). The margins of the upper and lower lids of one eye were trimmed and sutured together using a 5-0 suture kit with polyglycolic acid (CP Medical). Subjects were returned to their home cage after recovery at 37 °C for 1–2 hours and disqualified in the event of suture opening.

**Antibodies.** The following antibodies/dilutions were used: rabbit anti-estrogen receptor  $\alpha$  (ER $\alpha$ ; ThermoFisher, RRID: AB\_325813, 1:1000); mouse anti-estrogen receptor  $\beta$  (ER $\beta$ ; ThermoFisher; AB\_2717280, 1:1000); mouse anti-parvalbumin (PV; Millipore; RRID:AB\_2174013, 1:1000); mouse anti-Post Synaptic Density 95 kd (PSD95; ThermoFisher; RRID: AB\_325399, 1:200); rabbit anti-phospho- Serine 831-GluR1 (pS831; Sigma Aldrich; RRID:AB\_1977218, 1:1000); followed by appropriate secondary antibodies: goat anti-rabbit and anti-mouse IgG conjugated to Alexa-488 or 647 (Life Technologies; RRID:AB\_143165, RRID:AB\_2535805, 1:300). The specificity of the ER $\alpha$  antibody was validated by the vendor through immunolabeling in positive (ER $\alpha$ <sup>+</sup>/ER $\beta$ <sup>+</sup> T547D<sup>39,40</sup>) and negative cells (ER $\alpha$ <sup>-</sup>/ER $\beta$ <sup>-</sup> Hs578T<sup>41</sup>). We performed our own confirmation of the specificity of the ER $\beta$ , see results.

**Reagents.** HSV-H129 EGFP (strain 772; University of Pittsburgh Center for Neuroanatomy and Neurotropic Viruses (CNNV) and HSV-H129 mCherry (strain 373; CNNV) were diluted 1:1 with diH<sub>2</sub>O and 3  $\mu$ l was injected intraocularly (right eye: mCherry; left eye: EGFP) for anterograde delivery to primary visual cortex. 4',6-Diamidino-2'-phenylindole dihydrochloride (DAPI, Sigma; 1:10000) was used to visualize cell nuclei. Chondroitin sulfate proteoglycans (CSPGs) were visualized with fluorescein wisteria floribunda agglutinin (WFA, Vector Labs; 1:1000). 17 $\alpha$ -Estradiol ( $\alpha$ E2; Sigma Aldrich) was diluted to 15  $\mu$ g/kg in sesame oil (veh., Sigma Aldrich) and administered subcutaneously (s.c.) to awake subjects.

**Immunohistochemistry.** Subjects were perfused transcardially with phosphate buffered saline (PBS) followed by 4% paraformaldehyde (PFA) in PBS. The brain was post-fixed in 4% PFA for 24 hours followed by 30% sucrose for 48 hours and cryo-protectant solution (0.58 M sucrose, 30% (v/v) ethylene glycol, 3 mM sodium azide, 0.64 M sodium phosphate, pH 7.4) for 24 hours prior to sectioning. Coronal sections (40  $\mu$ m) were made on a Leica freezing microtome (Model SM 2000R). Sections (ML: 4 mm AP: -6.72 mm DV: 1.5 mm) were blocked with 4% normal goat serum (NGS) in PBS for 1 hour. Antibodies were presented in blocking solution for 24 hours,

followed by appropriate secondary antibodies for 2 hours. Immunolabeling for ER $\alpha$  and ER $\beta$  was absent when antibodies were pre- absorbed with antigen (*not shown*).

**Confocal imaging and analysis.** Images were acquired on a Zeiss LSM 710 confocal microscope. Tiled photomontages of ER $\alpha$ , ER $\beta$ , and ER $\alpha$ /ER $\beta$  with DAPI were constructed with MosaicJ (FIJI, NIH) from individual images (2.8 mm<sup>2</sup>) acquired at 5X magnification (Zeiss Plan-neofluar 5X/0.16, NA = 0.16). Co-localization of ER $\alpha$  and ER $\beta$  with DAPI was analyzed in single z-section images (70.86  $\times$  70.86  $\mu$ m, 550  $\mu$ m depth from cortical surface (corresponding to layer 4 of V1), 3 coronal sections/subject, 1 region of interest (ROI)/hemisphere) taken at 40X (Zeiss Plan-neofluar 40X/1.3 Oil DIC, NA = 1.3), using the JACoP plugin in FIJI (NIH). Pearson's correlation coefficient was used to calculate the covariance of two fluorescent signals independently of fluorescence intensity. HSV anterograde viral tracer signal was visualized in single z-section images (2.8 mm<sup>2</sup> or 1.4 mm<sup>2</sup>) acquired at 5X or 10X magnification (Zeiss Plan-neofluar 10x/0.30, NA = 0.30) and a mean intensity profile was calculated using FIJI. The cortical distribution of WFA and PV immunoreactivity was determined in a z-stack (9  $\times$  7.5  $\mu$ m sections, 3 coronal sections/subject, 1 ROI/hemisphere) acquired at 10X. Maximal intensity projections (MIPs; 500  $\mu$ m width, 900  $\mu$ m depth from cortical surface) were used to obtain mean intensity profiles in FIJI. For PSD95 and pS831 staining, MIPs of z-stacks (40 slices  $\times$  0.9  $\mu$ m images; 3 coronal sections/subject, 1 ROI/hemisphere) were acquired at 100X (Zeiss Plan-neofluar 100x/1.3 Oil DIC, NA = 1.3). PSD95 and pS831 puncta were selected using size exclusion parameters defined by unbiased quantification for each marker following the construction of a cumulative distribution of puncta size, and setting a 10% lower bound and 90% upper bound. In our acquisition setup, resolution ( $\lambda$ \*N.A.) = 200 nm, and our upper bound of 0.6 microns<sup>2</sup> is  $\sim$  3\*resolution. The lower limit is imposed to exclude subresolution, single pixels/stochastic noise from the analysis. Puncta were identified in MIPs (28.34  $\times$  28.34  $\times$  40  $\mu$ m z-stack images, 550  $\mu$ m depth from cortical surface) based on fluorescence thresholding (autothreshold) in FIJI, which allows image segmentation in micrographs with widely expressed fluorescence.

**Acute In Vivo Recordings.** Visually evoked potentials (VEPs) were recorded from the binocular region of primary visual cortex (V1b) of adult rats contralateral to the chronically deprived eye. Rats were anesthetized with 3% isoflurane in 100% O<sub>2</sub> and a 3 mm craniotomy was produced over V1b (centered 3 mm medial from midline and 7 mm posterior from Bregma). A 1.8 mm 16-channel platinum-iridium linear electrode array ( $\sim$ 112  $\mu$ m site spacing, 250 k $\Omega$ ) was inserted perpendicular to V1b (dorsal/ventral: 1.8 mm). Recordings under 2.5% isoflurane in 100% O<sub>2</sub> commenced 30 minutes after electrode insertion. Local field potentials were acquired via a RZ5 amplifier (Tucker Davis Technology) with a 300 Hz low pass filter and a 60 Hz notch filter. VEPs were evoked through passive viewing of 100  $\times$  1 second trials of square-wave gratings (0.05 cycles per degree (cpd), 100% contrast, reversing at 1 Hz, via MATLAB (Mathworks) with Psychtoolbox extensions. Average VEP waveforms were calculated for 100 stimulus presentations and were assigned to layers based on waveform shape. VEP amplitude was measured from trough to peak in MATLAB<sup>42</sup>. To examine the short-term plasticity of VEP amplitude, each eye was individually presented with full field flashes (90 cd/m<sup>2</sup>), alternating with 0 cd/m<sup>2</sup> every 0.5 seconds. Single trial VEP responses were normalized to the first evoked response. To examine the response of the amblyopic cortex to repetitive patterned visual stimulation, subjects received passive binocular stimulation of 200 phase reversals of 0.05 cycles per degree (cpd), 100% contrast gratings, 45 degrees, reversing at 1 Hz. After 24 hours, VEPs were evoked from each eye (originally deprived and non-deprived eye separately) in response to the familiar (45 degrees) and a novel (135 degrees) grating stimulus.

**Experimental Design and Statistical Analysis.** Primary visual cortex was defined with anatomical landmarks (dimensions of the dorsal hippocampal commissure, deep cerebral white matter tract, and the forceps major of the corpus callosum). Modest shrinkage due to fixation and cryoprotection reduced vertical depth to 900  $\mu$ m<sup>35</sup>. Fluorescent puncta were identified using size exclusion parameters defined by unbiased quantification for each marker following the construction of a cumulative distribution of puncta size, and setting a 10% lower bound and 90% upper bound. An unpaired two-tailed Student's T-test was used to probe the significance of differences between two independent experimental groups, and a paired Student's T-test was used for two measurements within the same subject. One-way ANOVA was used to determine significance between three independent groups. Repeated measures ANOVA, with between group comparisons, was used to probe the significance of differences between more than two measures within the same subjects, followed by a Tukey-Kramer honestly significant difference *post hoc* for pairwise comparisons if  $p < 0.05$  (JASP). A Kolmogorov-Smirnov test (K-S Test) was used to probe the significance between distributions of two independent data sets. Multi-dimensional K-S Test was used to probe the significance of differences between distributions with two independent measurements (MATLAB). Statistical significance ( $p < 0.05$ ) is represented as asterisks in figures and data is presented as mean  $\pm$  standard error (mean  $\pm$  SEM). Where statistical significance was observed ( $p < 0.05$ ) the effect size was calculated (Cohen's  $d$ ) as mean of group 1 mean - group 2 mean/combined standard deviation of groups 1 and 2, with  $d < 0.2$  considered a small effect,  $d > 0.2$ - $< 0.5$  considered medium and  $d > 0.8$  considered a large effect.

**Ethical approval Statement (duplicated in methods section).** All procedures were approved by the University of Maryland Institutional Animal Care and Use Committee and were carried out in accordance with the Guide for the Care and Use of Laboratory Animals.

## Results

**Effects of cMD on thalamocortical innervation of V1.** Estradiol (E2) treatment has been shown to promote short-term synaptic plasticity, increase the number and size of excitatory synapses, and lower the threshold for activity-dependent potentiation<sup>14,36,43</sup>. We therefore first asked how each of these potential targets of E2 is impacted in our animal model of amblyopia, in which chronic monocular deprivation (cMD) is imposed from

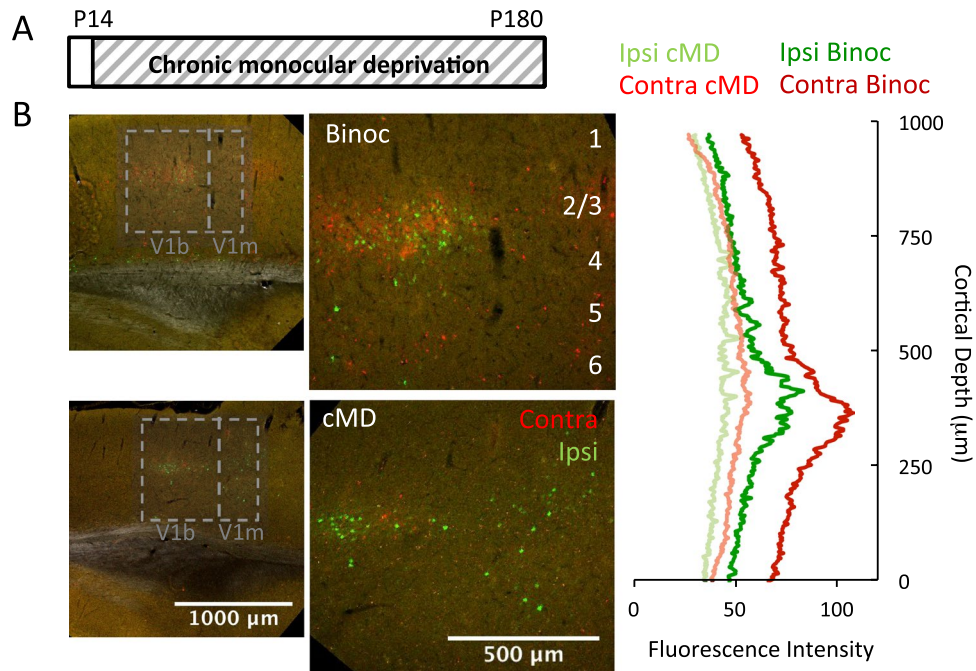


**Figure 1.** Chronic monocular deprivation decreases thalamic input to primary visual cortex. **(A)** Experimental timeline. Subjects received monocular deprivation from eye opening (~P14) to adulthood (>P180). **(B)** Left: Representative confocal double fluorescent micrographs of primary visual cortex (V1) following intravitreal delivery of H129 373, mCherry into right/contralateral and H129 772, EGFP into left/ipsilateral eye of a control binocular (top) and a cMD subject (bottom). V1 location (here and all other figures) ML: 4 mm AP:  $-6.72$  mm DV:  $1.5$  mm; ROI:  $2000\mu\text{m} \times 2000\mu\text{m}$ ; left:  $5\times$  mag with  $0.6\times$  digital zoom; right:  $900\mu\text{m} \times 1000\mu\text{m}$ ;  $10\times$  mag with  $0.6\times$  digital zoom). Right: Distribution of mCherry and EGFP fluorescence in V1b ( $900\times 100\mu\text{m}$  ROI, presented by vertical depth) of higher magnification images reveals a reduction in trans-neuronal label following cMD.

eye opening to adulthood (P14 - >P180). In binocular controls, twice as many thalamocortical afferents serve the contralateral as ipsilateral eye<sup>44</sup>, and neurons in the binocular region of primary visual cortex (V1b) prefer contralateral eye stimulation. A representative example of eye-specific innervation from the thalamus to the cortex, revealed by dual intraocular injection of the anterograde trans-neuronal label HSV-H129, confirms >1.5 fold innervation of layer 4 from the contralateral than the ipsilateral eye in binocular adult rats (Average Fluorescence  $\pm$  SEM; Ipsi HSV-EGFP  $54.61 \pm 0.22$ , Contra HSV-mCherry  $81.33 \pm 0.85$ ; Fig. 1B). Brief monocular deprivation shifts ocular preference away from the deprived eye and reduces the number of thalamic afferents serving the deprived eye innervating V1b<sup>45,46</sup>. Accordingly, cMD significantly decreases the thalamocortical innervation from the deprived contralateral eye, reducing the initial contralateral bias (average Fluorescence  $\pm$  SEM; Ipsi HSV-EGFP  $40.26 \pm 0.25$ , Contra HSV-mCherry  $47.38 \pm 0.22$ , Fig. 1B). cMD also induced an expansion of the cortical territory innervated by the non-deprived eye into the monocular region of V1 (V1m), as previously observed in felines<sup>47</sup>.

**Quantitative immunofluorescence of PSD95 and pS831 following cMD.** To ask if cMD impacted the number and/or size of excitatory synapses in the binocular region of primary visual cortex, we quantified the intensity and distribution of the scaffold protein PSD95. PSD95 is detected in nascent synaptic connections, and changes in PSD95 expression are correlated with changes in excitatory synaptic strength and number. Quantitative immunofluorescence revealed that cMD significantly reduced the size of PSD95 puncta in deprived and non-deprived V1b (Binoc versus deprived  $p < 0.001$ , K-S Test, Cohen's  $d = 0.51$ ; Binoc versus non-deprived,  $p < 0.001$ , K-S Test, Cohen's  $d = 0.39$ ) that was similar in males and females ( $F(1,16) = 0.29$ ,  $p = 0.87$ , 2-way ANOVA). However, we observed no difference in the average number of PSD95 puncta in V1b contralateral or ipsilateral to the chronically-deprived eye (AVG  $\pm$  SEM; Binocular Control (Binoc)  $333.36 \pm 44.19$ , Contralateral (Contra cMD)  $320.65 \pm 54.46$ , Ipsilateral (Ipsi cMD)  $297.87 \pm 53.71$ ; males versus females:  $F(1,16) = 0.76$ ,  $p = 0.14$ , 2-way ANOVA;  $n = 8$ , Fig. 2A).

To ask if cMD impacted the activity of signaling pathways known to regulate glutamate receptor function, we examined the density and distribution of the GluA1 subunit of the  $\alpha$ -amino-3-hydroxy-5-methyl-4-isoxazolepropionic acid receptor subtype of glutamate receptor (AMPA) phosphorylated on residue Serine 831 (pS831).  $\text{Ca}^{2+}$ /calmodulin-dependent protein kinase II (CaMKII) and protein kinase C (PKC)-dependent phosphorylation of Serine 831 of the GluA1 subunit increases single channel conductance and promotes LTP<sup>48</sup>. Importantly, rapid and transient phosphorylation of pS831 is induced *in vivo* by salient stimulation<sup>49,50</sup>. However, following cMD, we observed no difference in the distribution of size or average number of pS831 puncta in V1b

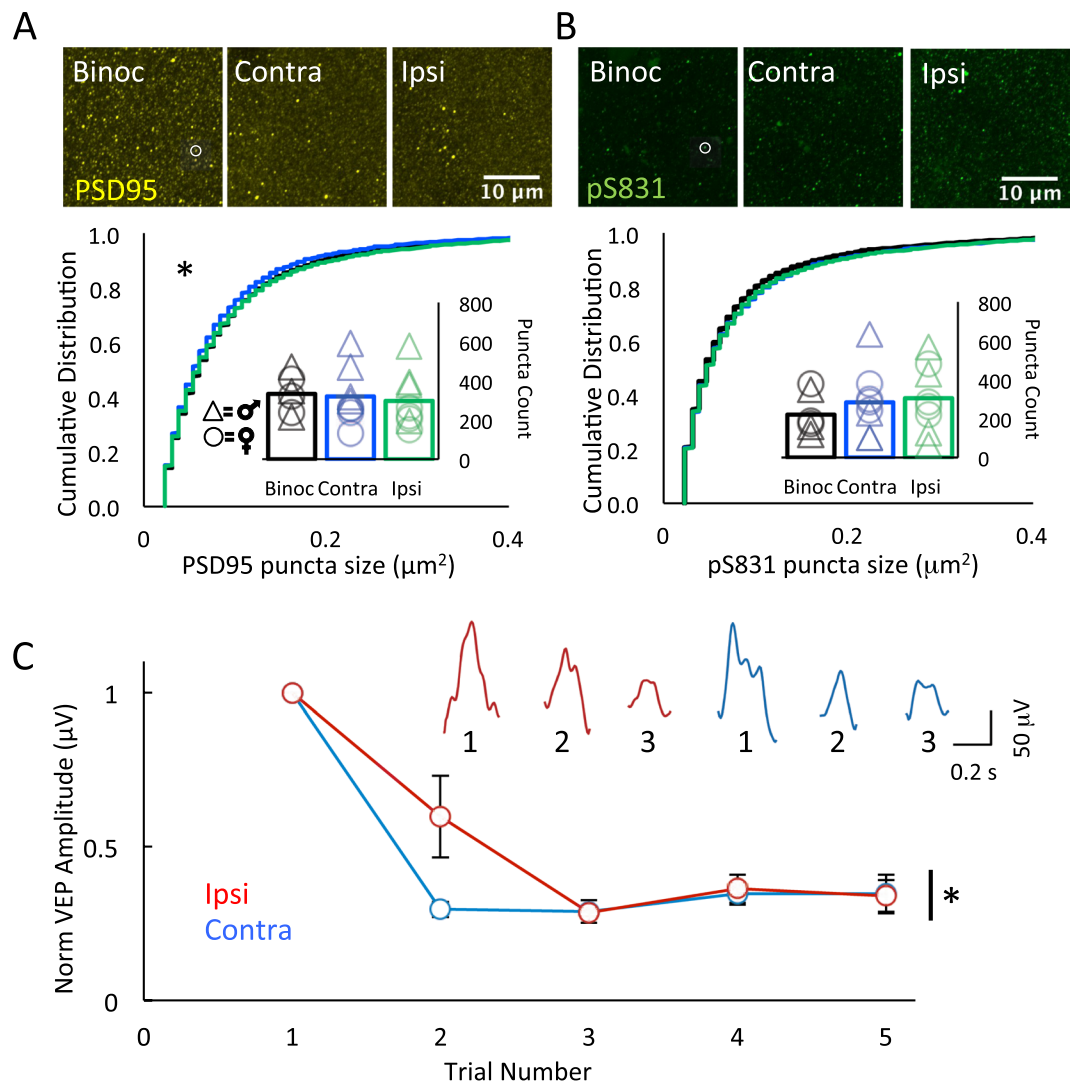


**Figure 2.** Chronic monocular deprivation decreases the size of PSD95 puncta and regulates the response to repetitive visual stimulation. **(A)** Top: Fluorescent micrographs of PSD95 (yellow, representative punctum in white circle) in V1b of binocular control (Binoc, left) and following cMD (Contra cMD, middle; Ipsi cMD, right). ROI 500 μm from surface; 28.34 μm × 28.34 μm × 40 μm, 100x mag with 3x digital zoom; maximal intensity projection (MIP; 40 × 1 μm z-steps). Bottom: Significant decrease in PSD95 immunoreactive puncta size in V1b following cMD \* $p < 0.001$ , K-S Test Contra and Ipsi relative to Binoc. No change in puncta number (inset). Males (triangles) vs. females (circles): 2-way ANOVAs size:  $F(1,16) = 0.29$ ,  $p = 0.87$ ; number:  $F(1,16) = 0.76$ ,  $p = 0.14$ , 2-way ANOVA; Binoc  $n = 3$  males, 3 females, cMD  $n = 4$  males, 4 females. **(B)** Top: Fluorescent micrographs of pS831 (green, representative punctum in white circle) in V1b of binocular control (Binoc, left) and following cMD (Contra cMD, middle; Ipsi cMD, right). ROI as in 2A. Bottom: No change in pS831 immunoreactive puncta size or number (inset) in V1b following cMD. Males (triangles) vs. females (circles): 2-way ANOVA Size:  $F(1,16) = 0.17$ ,  $p = 0.69$ ; Number:  $F(1,16) = 0.29$ ,  $p = 0.87$ ; Binoc  $n = 3$  males, 3 females, cMD  $n = 4$  males, 4 females. **(C)** VEPs acquired from layer 2/3 *in vivo* in response to single full field light flash to ipsilateral (non-deprived, red) and contralateral eye (deprived, blue) normalized to the amplitude of the first response. Contralateral eye VEPs depress more rapidly than ipsilateral eye VEPs. Inset: representative raw, single VEP waveforms in response to 3 consecutive light flashes (full field, 0.5 second 90 cd/m<sup>2</sup>, 0.5 second 0 cd/m<sup>2</sup>) to ipsilateral (red) and contralateral (blue) eyes. Second VEP amplitude normalized to first, AVG ± SEM; Ipsi:  $0.59 \pm 0.13$ , Contra:  $0.29 \pm 0.02$ ; Repeated measures ANOVA, \* $p < 0.001$ ,  $F = 47.683$ , between groups,  $p = 0.007$ ,  $F = 15.773$ ,  $n = 4$  subjects.

contralateral or ipsilateral to the occluded eye (pS831 puncta size: Binoc versus deprived  $p > 0.05$ , K-S Test; Binoc versus non-deprived,  $p > 0.05$ ; Males versus females:  $F(1,16) = 0.17$ ,  $p = 0.69$ , 2-way ANOVA; pS831 puncta number AVG ± SEM: Binoc  $227.82 \pm 48.40$ , Contra cMD  $283.68 \pm 64.10$ , Ipsi cMD  $305.01 \pm 66.20$ . Males versus females:  $F(1,16) = 0.78$ ,  $p = 0.39$ , 2-way ANOVA; Binoc  $n = 6$ , cMD  $n = 8$ , Fig. 2B). The absence of change in total excitatory synapses density despite the reduction in thalamic input to the cortex implicates an increase in the density of other classes of excitatory synapses following cMD.

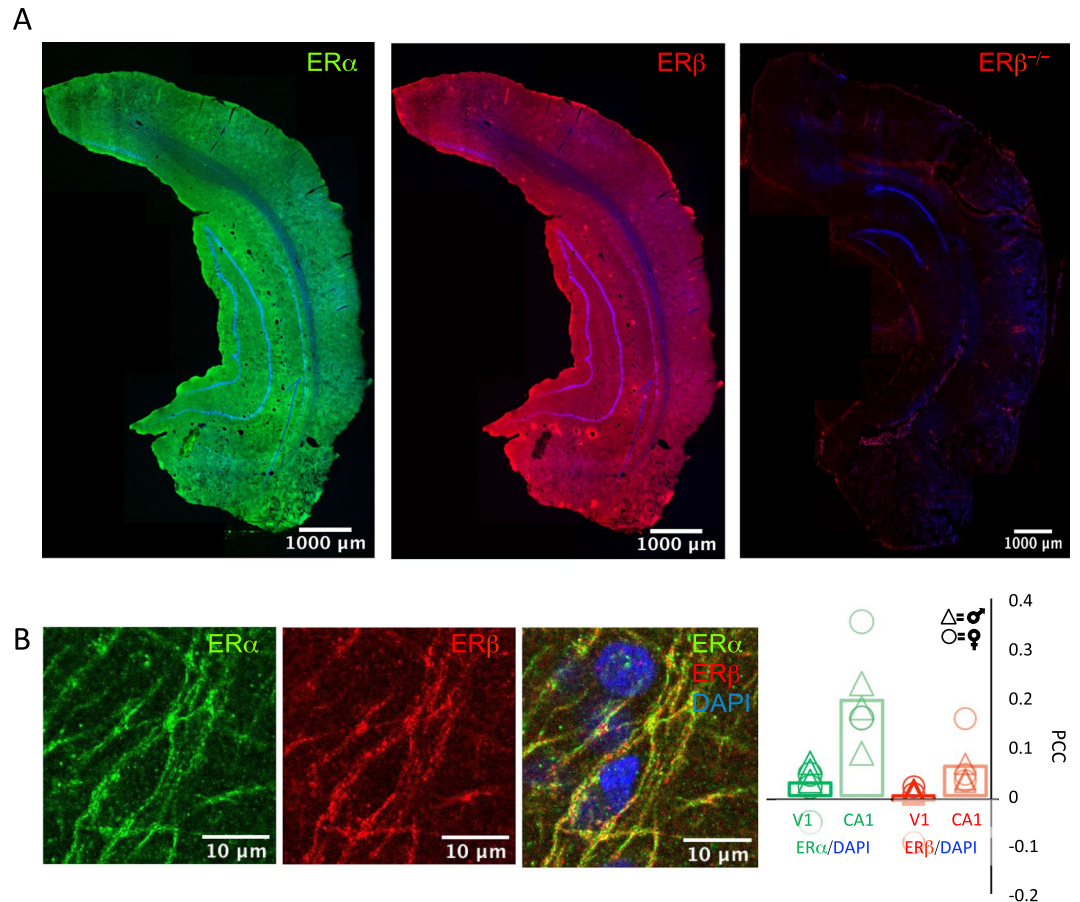


**Figure 3.** Distribution of estrogen receptors ER $\alpha$  and ER $\beta$  in adult male and female rat brains. **(A)** Low magnification single z-section fluorescent micrographs of coronal plane of adult rats. Immunoreactivity for ER $\alpha$  (left; green) and ER $\beta$  (middle; red) in adult male WT and immunoreactivity for ER $\beta$  in adult female ER $\beta^{-/-}$ , counter-stained with DAPI (blue). 5X magnification, ROI 129.17  $\mu\text{m} \times 129.17 \mu\text{m}$ . **(B)** Higher magnification single z-section fluorescent micrographs of triple labeled ER $\alpha$  (green, left)/ER $\beta$  (red, middle) and DAPI (blue, right). ROI: V1b 500  $\mu\text{m}$  from surface: 72  $\mu\text{m} \times 82 \mu\text{m}$ ; 40x mag plus 3x digital zoom. Same subjects as in **(A)**. Pearson's correlation coefficient (PCC) reveals low correlation between nuclear signal (DAPI) and ER $\alpha$  (green) and ER $\beta$  (red) in adult male and female WT rats in V1 (dark green, dark red) and CA1 (light green, light red). Males (triangles) vs. females (circles): student's t-test: V1 DAPI-ER $\alpha$   $p = 0.21$ , DAPI-ER $\beta$ :  $p = 0.43$ , CA1 DAPI-ER $\alpha$ :  $p = 0.48$ , DAPI-ER $\beta$ :  $p = 0.44$ ;  $n = 3$  males, 3 females.

**VEP responses following cMD.** To ask if cMD impacted short-term activity-dependent synaptic plasticity, we examined changes in the amplitude of visually evoked local field potentials (VEPs) in response to repetitive visual stimulation of each eye. Microelectrode array recordings of the VEP isolated from layer 2/3 of V1b contralateral to the occluded eye (deprived hemisphere) were acquired in response to repetitive flash stimuli (full field, 0.5 second 90  $\text{cd}/\text{m}^2$ , 0.5 second 0  $\text{cd}/\text{m}^2$ ) and amplitudes were normalized to the first VEP. Full field flashes of light were used to maximally stimulate synapses in the amblyopic cortex, as chronic monocular deprivation is known to severely compromise spatial acuity<sup>33,35,51</sup>. Responses were assigned to cortical layer by the shape of the VEP waveform, a reliable indicator of laminar location that is independent of variables associated with electrode fabrication and placement. Repetitive visual stimulation revealed that activity-dependent depression of VEP amplitudes was accelerated following deprived/contralateral eye stimulation relative to non-deprived/ipsilateral eye stimulation (Second VEP response normalized to first,  $\text{AVG} \pm \text{SEM}$ ; Ipsi  $0.59 \pm 0.13 \mu\text{V}$ , Contra  $0.29 \pm 0.02 \mu\text{V}$ ; Repeated measures ANOVA,  $p < 0.001$ ,  $F = 47.683$ , between groups,  $p = 0.007$ ,  $F = 15.773$ , Cohen's  $d = 2.31$ ,  $n = 4$  subjects, Fig. 2C). The acceleration of short-term synaptic depression of VEP amplitude suggests that cMD induces an increase in the neurotransmitter release probability at synapses serving the deprived eye, similar to the response to brief MD in the thalamus and visual cortex<sup>52,53</sup>.

**ERs in adult rodent V1.** To ask if the adult visual cortex has the potential to respond to estrogen treatment, we examined the distribution of canonical ERs. Our examination was performed in adult ( $>P180$ ), gonadally-intact, male and female LE rats, as gonadectomy significantly reduces excitatory synaptic density<sup>11,12,54</sup>. Quantitative immunohistochemistry reveals robust expression of ER $\alpha$  and ER $\beta$  throughout the brains of adult males and females (Fig. 3A). To ask if ERs in the adult brain are located outside of the nucleus, we compared the

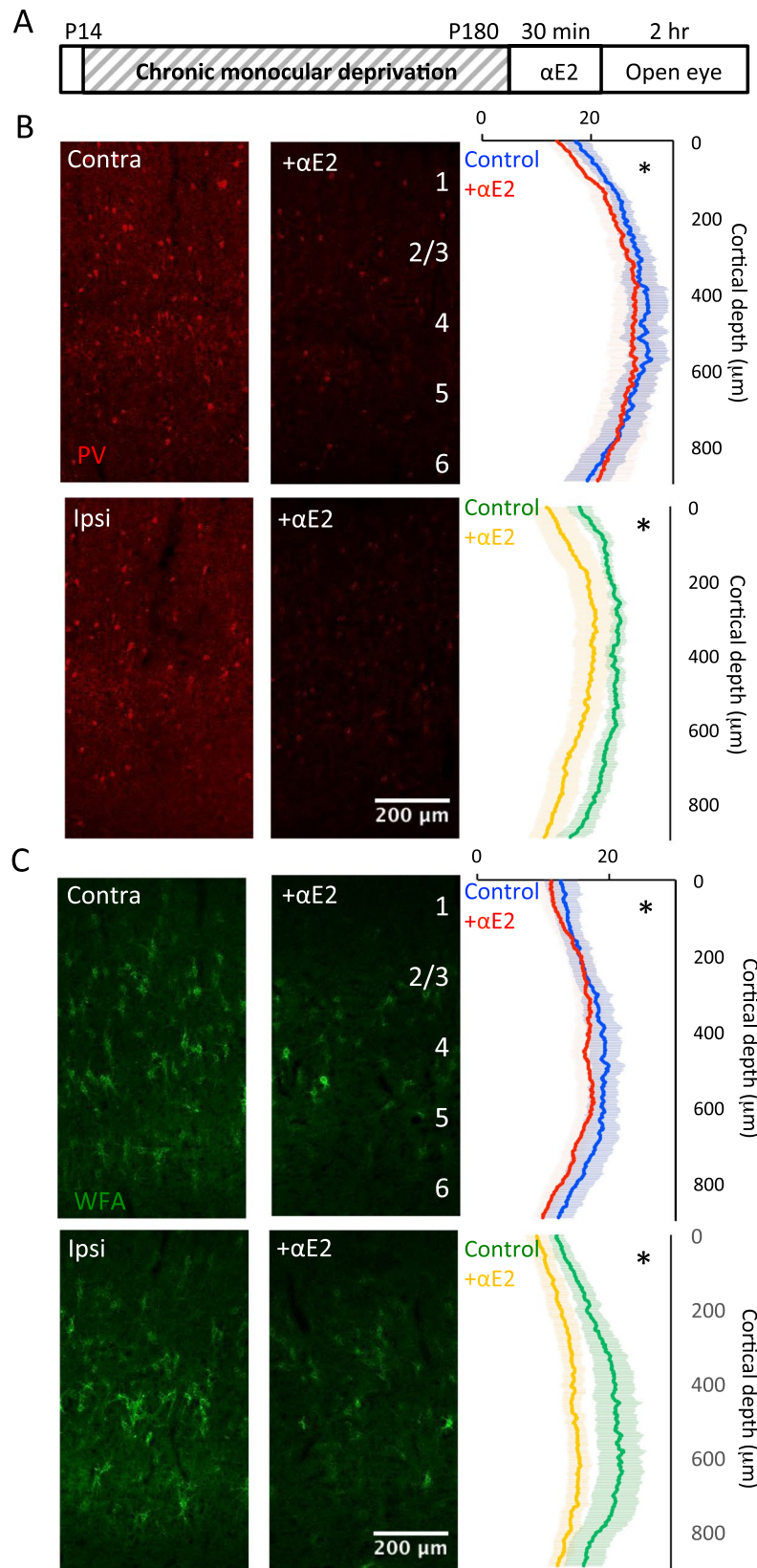


**Figure 4.** Acute  $17\alpha$ -estradiol treatment reduces PV and WFA staining in V1b contralateral and ipsilateral to cMD. **(A)** Experimental timeline. Subjects received monocular deprivation from eye opening ( $\sim$ P14) to adulthood ( $>$ P180).  $17\alpha$ -estradiol ( $15\mu\text{g}/\text{kg}$ , s.c.) was delivered 30 minutes prior to eye opening. **(B)** Left: Fluorescent micrographs of PV distribution in V1b (red; ROI:  $900\mu\text{m} \times 500\mu\text{m}$ ;  $10\times$  mag; MIP;  $9 \times 7.5\mu\text{m}$  sections). Right: Average  $\pm$  SEM PV fluorescence intensity in ROI by vertical depth.  $17\alpha$  estradiol significantly decreases PV fluorescence intensity in V1b contralateral and ipsilateral to cMD \* $p < 0.001$ , K-S Test. Males

versus females: 2-way ANOVA Contra:  $F(1,8) = 4.39$ ,  $p = 0.07$ ; Ipsi:  $F(1,8) = 0.41$ ,  $p = 0.54$ ;  $n = 6$  each. (C) Left: Fluorescent micrographs of WFA distribution in V1b (green; ROI as in 3b). Right: Average  $\pm$  SEM WFA fluorescence intensity in ROI by vertical depth.  $17\alpha$ -estradiol significantly decreases WFA intensity in V1b contralateral and ipsilateral to cMD =  $p < 0.001$ , K-S Test. Males versus females: 2-way ANOVA Contra:  $F(1,8) = 3.23$ ,  $p = 0.11$ ; Ipsi:  $F(1,8) = 1.69$ ,  $p = 0.23$ ;  $n = 6$  each.

distribution of ER $\alpha$  and ER $\beta$  to the distribution of DAPI (4',6-Diamidino-2'-phenylindole dihydrochloride), a fluorescent stain that binds to AT-rich sequences of DNA. Pearson's correlation coefficients (PCC) reveal low co-localization between DAPI/ER $\alpha$  and DAPI/ER $\beta$  in V1 of adult males and females (AVG  $\pm$  SEM; DAPI-ER $\alpha$ : Males  $0.048 \pm 0.023$ , Females  $0.002 \pm 0.037$ , males vs. females  $p = 0.21$ , student's t-test; DAPI-ER $\beta$ : Males  $0.006 \pm 0.024$ , Females:  $-0.025 \pm 0.037$ , males vs. females  $p = 0.43$ , student's t-test;  $n = 3$  males and  $n = 3$  females; Fig. 3B). Low co-localization between DAPI and ER $\alpha$  and ER $\beta$  was also observed in hippocampal area CA1 of these same subjects, in agreement with previous reports<sup>23,24</sup> (AVG  $\pm$  SEM; DAPI-ER $\alpha$ : Males  $0.163 \pm 0.041$ , Females  $0.223 \pm 0.06$ , males vs. females,  $p = 0.48$ , student's t-test; DAPI-ER $\beta$ : Males  $0.042 \pm 0.011$ , Females:  $0.076 \pm 0.039$ ; males vs. females  $p = 0.44$ , student's t-test,  $n = 3$  males and  $n = 3$  females; Fig. 3B). Immunolabeling for ER $\alpha$  and ER $\beta$  was absent when antibodies were pre-absorbed with antigen (*not shown*), and ER $\beta$  staining was absent in the brains of ER $\beta^{-/-}$  adult female rats (Representative example of  $n = 3$ ; Fig. 2A, right<sup>38</sup>). This extends the list of brain regions of the rat that maintain robust non-nuclear expression of ERs in adulthood to the primary visual cortex.

The structural and functional deficits induced by prolonged monocular deprivation do not recover spontaneously following removal of the occlusion in adulthood<sup>33,45</sup>. However, recovery of vision in the amblyopic pathway can be promoted by manipulations that enhance synaptic plasticity in V1b<sup>35,55–58</sup>. To ask if estrogen treatment can enhance structural and functional plasticity in the adult amblyopic V1, we treated with  $17\alpha$ -estradiol ( $\alpha$ E2), a stereoisomer of the main circulating estradiol (E2), which induces potent synaptogenesis but is genomically inactive<sup>36</sup>. To confirm the latter, we found that 7 days of  $\alpha$ E2 treatment ( $15\mu\text{g}/\text{kg}$ , s.c., 1x/day, awake animals) to adult females and males resulted in no change in gonad/body weight (AVG  $\pm$  SEM; female vehicle (veh):  $4.10 \pm 0.38$  vs. female  $\alpha$ E2:  $5.134 \pm 1.09$ ; male veh:  $6.01 \pm 0.90$  vs. male E2:  $5.59 \pm 0.34$ , males  $n = 3$ , females  $n = 3$ ).

**Effect of  $\alpha$ E2 on anatomical markers of plasticity.** To ask if acute  $\alpha$ E2 treatment regulates neuronal function in the amblyopic visual cortex, we examined the response to a single dose of  $\alpha$ E2 on the expression of the activity-dependent calcium-binding protein parvalbumin (PV), a proxy for the activity of fast-spiking interneurons (FS INs<sup>59</sup>). A dose of  $\alpha$ E2, previously shown to induce potent structural plasticity ( $15\mu\text{g}/\text{kg}$ , s.c.<sup>36</sup>), was delivered to awake amblyopic male and female rats.  $\alpha$ E2 treatment induced a decrease in the size distribution of PV immunofluorescent puncta in V1b contralateral and ipsilateral to the occluded eye (AVG  $\pm$  SEM; Contra cMD  $26.18 \pm 2.67$  vs. Contra cMD +  $\alpha$ E2  $24.68 \pm 3.61$ ,  $p < 0.001$ , K-S Test, Cohen's  $d = 0.47$ ; males vs. females, 2-way ANOVA  $F(1,8) = 4.39$ ,  $p = 0.07$ ; Ipsi cMD  $25.59 \pm 1.42$  vs. Ipsi cMD +  $\alpha$ E2  $18.97 \pm 3.17$ ;  $p < 0.001$ , K-S Test, Cohen's  $d = 2.69$ ; males vs. females 2-way ANOVA  $F(1,8) = 0.41$ ,  $p = 0.54$ ;  $n = 6$ , each; Fig. 4A,B). This suggests a reduction in the excitability of PV INs, and a subsequent disinhibition of PV IN targets, which may underlie observations that E2 treatment increases principal neuron excitability<sup>60–62</sup>.

Next, we examined the effect of  $\alpha$ E2 on the integrity of the extracellular matrix (ECM), the maturation of which contributes to the constraint of structural and functional plasticity with age<sup>63,64</sup>. Chondroitin sulfate proteoglycans (CSPGs), a primary component of the ECM, are labeled by Wisteria-floribunda agglutinin (WFA) binding to N-acetyl-D-galactosamine in the chondroitin sulfate chain.  $\alpha$ E2 treatment of cMD subjects ( $15\mu\text{g}/\text{kg}$ , s.c.) induced a decrease in the distribution of fluorescein-WFA staining in V1b contralateral and ipsilateral to the occluded eye (Contra cMD vs. Contra  $\alpha$ E2,  $p < 0.001$  K-S Test, Cohen's  $d = 0.91$ ; males versus females:  $F(1,8) = 3.23$ ,  $p = 0.11$ , 2-way ANOVA; Ipsi cMD vs. Ipsi  $\alpha$ E2,  $p < 0.001$  K-S Test, Cohen's  $d = 2.48$ ; males versus females:  $F(1,8) = 1.69$ ,  $p = 0.23$ , 2-way ANOVA;  $n = 6$ , Fig. 4C,D). Thus,  $\alpha$ E2 treatment induces changes in the adult amblyopic cortex that are predicted to promote synaptic plasticity.

**Quantitative immunofluorescence of PSD95 and pS831 following  $\alpha$ E2.** To ask if  $\alpha$ E2 treatment impacts the density of excitatory synapses, we again examined the intensity and distribution of PSD95 labeling.  $\alpha$ E2 treatment of cMD subjects ( $15\mu\text{g}/\text{kg}$ , s.c.) induced a significant increase in the size of PSD95 immunoreactive puncta in V1b contralateral, but not ipsilateral, to the occluded eye in males and females (Contra cMD vs. Contra  $\alpha$ E2,  $p < 0.001$  K-S Test, Cohen's  $d = 0.13$ ; males versus females:  $F(1,2) = 0.98$ ,  $p = 0.34$ , 2-way ANOVA; Ipsi cMD vs. Ipsi  $\alpha$ E2; males vs. females,  $F(1,12) = 0.11$ ,  $p = 0.75$ , 2-way ANOVA), but no change in PSD95 number (AVG  $\pm$  SEM; Contra cMD  $320.65 \pm 54.46$  vs. Contra  $\alpha$ E2  $364.03 \pm 47.96$ ; males vs. females,  $F(1,12) = 1.84$ ,  $p = 0.95$ , 2-way ANOVA; Ipsi cMD  $297.87 \pm 53.71$  vs. Ipsi  $\alpha$ E2  $389.46 \pm 64.07$ ; males vs. females,  $F(1,12) = 4.27$ ,  $p = 0.06$ , 2-way ANOVA;  $n = 8$  each, Fig. 5B). In contrast, we observed a decrease in the size of pS831 immunoreactive puncta in both hemispheres following  $\alpha$ E2 treatment (AVG  $\pm$  SEM; Contra cMD vs. Contra  $\alpha$ E2,  $p < 0.001$  K-S Test, Cohen's  $d = 1.37$ ; males versus females:  $F(1,12) = 0.138$ ,  $p = 0.72$ , 2-way ANOVA; Ipsi cMD vs. Ipsi  $\alpha$ E2,  $p < 0.001$ , K-S Test, Cohen's  $d = 0.18$ ; males versus females:  $F(1,12) = 0.01$ ,  $p = 0.91$ , 2-way ANOVA) but no change in puncta number following  $\alpha$ E2 treatment (Contra cMD  $283.68 \pm 64.10$  vs. Contra  $\alpha$ E2  $359.06 \pm 69.38$ ; males versus females:  $F(1,12) = 1.38$ ,  $p = 0.26$ , 2-way ANOVA; Ipsi cMD  $305.01 \pm 66.20$  vs. Ipsi  $\alpha$ E2  $358.53 \pm 70.82$ ; males versus females:  $F(1,12) = 2.16$ ,  $p = 0.17$ , 2-way ANOVA;  $n = 8$ , Fig. 5C). This suggests that  $\alpha$ E2 treatment increases the size of existing excitatory synapses in the adult V1 via a pathway that is independent of CaMKII/PKC phosphorylation of GluA1.



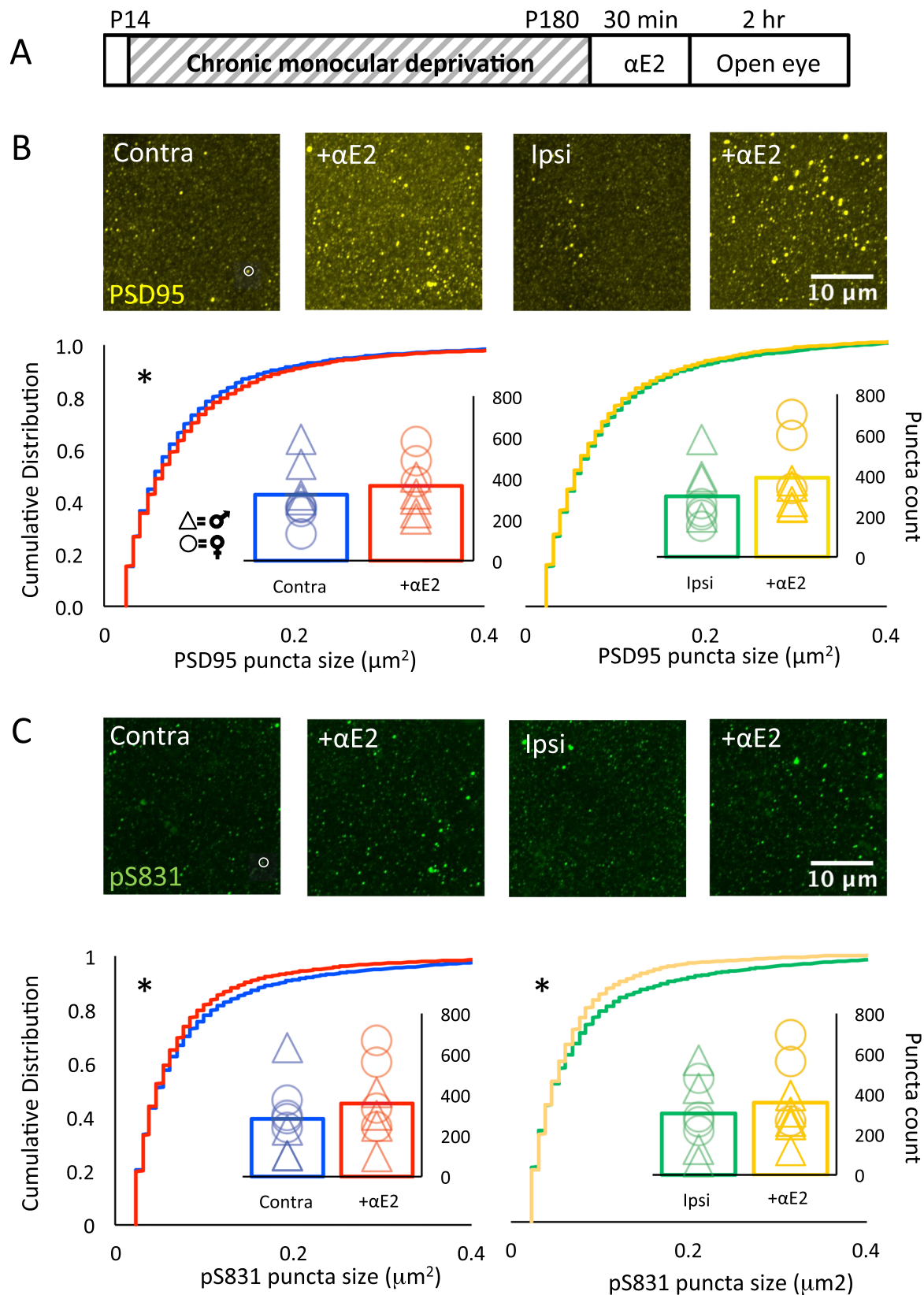


**Figure 5.** Acute 17 $\alpha$ -estradiol treatment increases PSD95 and decreases pSer831 puncta size. **(A)** Experimental timeline. Subjects received monocular deprivation from eye opening (~P14) to adulthood (>P180). 17 $\alpha$ -estradiol (15  $\mu$ g/kg, s.c.) was delivered 30 minutes prior to eye opening. **(B)** Top: Fluorescent micrographs of PSD95 immunoreactivity (yellow, representative punctum in white circle) in V1b  $\pm$  17 $\alpha$  estradiol contralateral (left) and ipsilateral (right) to cMD (V1b; 500  $\mu$ m from surface; ROI: 28.34  $\mu$ m  $\times$  28.34  $\mu$ m  $\times$  40  $\mu$ m, 100x mag with 3x digital zoom; MIP; 40  $\times$  1  $\mu$ m z-steps). Bottom: Cumulative

distribution reveals a significant increase in PSD95 immunoreactive puncta size in V1b contralateral (left), but not ipsilateral (right) to the deprived eye,  $*p < 0.001$ , K-S Test. Males (triangles) vs. females (circles): 2-way ANOVA Contra:  $F(1,12) = 0.98$ ,  $p = 0.34$ , Ipsi:  $F(1,12) = 0.11$ ,  $p = 0.75$ . No change in PSD 95 immunoreactive puncta number (insets). Males (triangles) vs. females (circles): 2-way ANOVA Contra:  $F(1,12) = 1.84$ ,  $p = 0.95$ , Ipsi:  $F(1,12) = 4.27$ ,  $p = 0.06$ ,  $n = 8$ . (C) Top: Fluorescent micrographs of pS831 immunoreactivity (green, representative punctum in white circle) in V1b  $\pm 17\alpha$ -estradiol contralateral (left) and ipsilateral (right) to cMD. ROI as in 4b. Bottom: Cumulative distribution reveals a significant decrease in pS831 immunoreactive puncta size in V1b contralateral (left) and ipsilateral (right) to the deprived eye,  $*p < 0.001$ , K-S Test. Males (triangles) vs. females (circles): 2-way ANOVA Contra:  $F(1,12) = 0.138$ ,  $p = 0.72$ ; Ipsi:  $F(1,12) = 0.01$ ,  $p = 0.91$ . No change in pS831 immunoreactive puncta number (insets). Males (triangles) vs. females (circles): 2-way ANOVA Contra:  $F(1,12) = 1.38$ ,  $p = 0.26$ , Ipsi:  $F(1,12) = 2.16$ ,  $p = 0.17$ ,  $n = 8$ .

**Effect of  $\alpha$ E2 on experience-dependent synaptic plasticity in cMD subjects.** To ask if  $\alpha$ E2 treatment could enhance functional plasticity in adult amblyopic V1, we adapted a visual stimulation protocol known to induce stimulus-selective response potentiation (SRP) of visual responses in binocular mice<sup>65</sup>. Repetitive presentation of oriented high contrast gratings (200–500 phase reversals a day over 5–7 days) induces a two-fold increase in the amplitude of the VEP recorded in layer 4 in juvenile or young adult, but not aged, mice<sup>66</sup>. The visual response potentiation is highly selective for the characteristic of the familiar visual stimulus including orientation, thereby reproducing the specificity of many forms of visual perceptual learning. In addition, our previous work has demonstrated that a truncated stimulation protocol, in which subjects receive 100–200 phase reversals of a high contrast grating, can be used to probe the level of plasticity available to cortical synapses. Indeed, the truncated protocol is insufficient to induce stimulus-selective response potentiation (SRP) in anesthetized amblyopic rats<sup>67</sup>, but robust SRP is induced following manipulations to enhance plasticity in the visual cortex<sup>67</sup>. To ask if the amblyopic visual cortex expresses SRP in response to this protocol following  $\alpha$ E2 treatment, we presented repetitive visual stimulation binocularly (200 phase reversal of 0.05 cycles per degree (cpd), 100% contrast gratings, 45 degrees, reversing at 1 Hz). After 24 hours, we compared monocular VEP amplitudes in response to the familiar and novel grating orientations (45 and 135 degrees respectively) in subjects with and without  $\alpha$ E2 treatment. As expected, we observed no potentiation of the amplitude of the VEP acquired from the previously deprived or non-deprived eye in vehicle-treated controls (AVG  $\pm$  SEM; non-deprived, familiar:  $22.37 \pm 1.28 \mu\text{V}$ , novel:  $22.71 \pm 2.55 \mu\text{V}$ ; males versus females:  $F(1,4) = 1.09$ ,  $p = 0.36$ , 2-way ANOVA; deprived, familiar:  $21.65 \pm 3.59 \mu\text{V}$ , novel:  $19.99 \pm 3.36 \mu\text{V}$ ; males versus females:  $F(1,4) = 1.19$ ,  $p = 0.34$ , 2-way ANOVA;  $n = 4$ , Fig. 6B,C). However,  $\alpha$ E2 treatment prior to the initial visual stimulation enabled significant potentiation of the response evoked by stimulation of the non-deprived eye (AVG  $\pm$  SEM; familiar:  $36.10 \pm 6.38 \mu\text{V}$ , novel:  $27.11 \pm 4.93 \mu\text{V}$ ;  $*p = 0.024$  two-tailed paired t-test, Cohen's  $d = 0.13$ ; males versus females:  $F(1,8) = 2.05$ ,  $p = 0.19$ , 2-way ANOVA;  $n = 6$  subjects, Fig. 6B). Importantly, the increase in the amplitude of the non-deprived eye VEP was stimulus-selective, as the increase was observed in response to familiar, but not novel, visual stimulus orientations (Fig. 6B). In contrast,  $\alpha$ E2 treatment did not enable potentiation of the VEP acquired from the previously deprived eye (AVG  $\pm$  SEM; familiar:  $25.56 \pm 4.49 \mu\text{V}$ , novel:  $29.154 \pm 3.80 \mu\text{V}$ ; males vs. females,  $F(1,8) = 1.59$ ,  $p = 0.24$ , 2-way ANOVA;  $n = 6$ , Fig. 6C). Thus  $\alpha$ E2 treatment specifically enhances plasticity of the spared synapses serving the non-deprived eye.

## Discussion

The enhancement of structural and functional plasticity by E2 is well-documented in adult hippocampus, hypothalamus and frontal cortex<sup>2,7,11,68,69</sup>. Here we demonstrate that the amblyopic visual cortex of adult rats retains sensitivity to estradiol treatment. A single dose of  $\alpha$ E2 reduced the expression of PV, reduced the integrity of the ECM, and increased the expression of the postsynaptic scaffold PSD95. Furthermore,  $\alpha$ E2 treatment promoted the induction of stimulus-selective response potentiation in the pathway served by the non-deprived eye. Our results demonstrate that a single acute treatment with  $\alpha$ E2 can regulate the structure and function of the adult visual cortex, and suggests that the sensitivity to acute  $\alpha$ E2 may be determined by synaptic properties that reflect the history of activity at the synapse.

We have previously shown that cMD induces a severe asymmetry in the structure and function of the cortical circuitry serving the deprived eye versus non-deprived eye<sup>33,35,66</sup>. The cMD model therefore allowed us to compare the response to acute  $\alpha$ E2 treatment in the severely compromised deprived eye pathway and the relatively intact non-deprived eye pathway in the same subjects. Intraocular delivery of a trans-neuronal tracer following cMD revealed the expected decrease in thalamocortical inputs serving the deprived eye, consistent with the significant depression in the strength of thalamic input to the cortex following MD<sup>45</sup>. Nonetheless, normal PSD95 and pS831 labeling was observed in the binocular regions of primary visual cortex after cMD, suggesting an increase in other classes of excitatory synapses following the loss of thalamocortical inputs. Indeed, MD during the critical period induces a rapid depression of deprived eye responses followed by a slowly emerging enhancement of non-deprived eye responses<sup>46</sup>. The expansion of thalamocortical input into V1m may also contribute to the increase in non-deprived eye response strength.

The therapeutic potential of E2/ $\alpha$ E2 in adults critically depends on the distribution and concentration of ERs in the brain. The persistence of robust, non-nuclear ER expression after menopause/estropause is well documented in primate and rodent hippocampus, hypothalamus, and frontal cortex. However, there has been little consensus on the distribution or role of ERs in adult primary sensory cortices<sup>29–32,48</sup>. Our results demonstrate that robust ER $\alpha$  and ER $\beta$  expression persists V1 of adult male and female LE rats. The majority of ER $\alpha$  and ER $\beta$

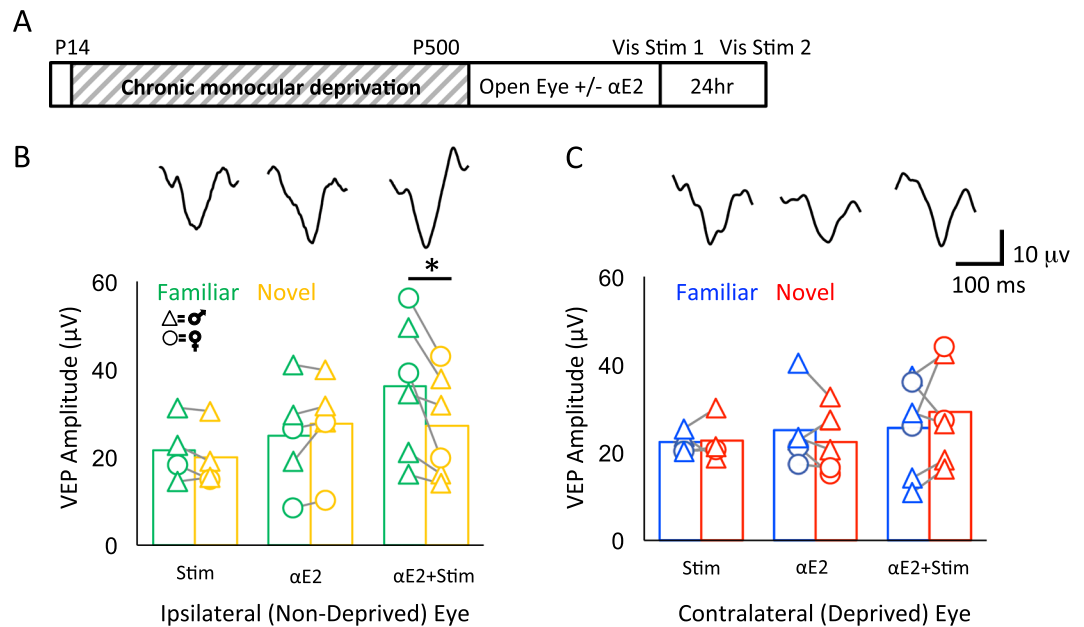


**Figure 6.** Acute  $17\alpha$ -estradiol promotes stimulus-selective response potentiation (SRP) of the non-deprived eye VEP. **(A)** Experimental timeline. Subjects received monocular deprivation from eye opening ( $\sim$ P14) to adulthood ( $>$ P180).  $17\alpha$ -estradiol ( $15\mu\text{g}/\text{kg}$ , s.c.) was delivered 30 minutes prior to opening the deprived eye and initial binocular visual stimulation (200 phase reversals at 1 Hz of 0.05 cycle per degree 100% contrast gratings at 45 degrees). VEPs were acquired from layer 4 in response to familiar (45 degrees) and novel (135 degrees) grating orientations 24 hours after the initial visual stimulus. **(B)** Average VEP amplitude evoked by stimulation of the ipsilateral (non-deprived) eye in response to familiar (green) and novel (yellow) visual stimuli. No difference in response to familiar versus novel stimuli in subjects that received visual stimulation or  $\alpha\text{E2}$  alone. Significant increase in response to familiar versus novel visual stimulus in subjects that received  $\alpha\text{E2}$  prior to initial visual stimulation. Inset: representative VEP waveforms in response to the familiar stimulus in vis stim only (left)  $\alpha\text{E2}$  only (center) and  $\alpha\text{E2}$  + vis stim (right). \* $p < 0.05$ , two-tailed paired t-test. Stim  $n = 4$ ,  $\alpha\text{E2}$   $n = 5$ ,  $\alpha\text{E2}$  + Stim  $n = 6$ . Males (triangles) vs. females (circles): 2-way ANOVA  $F(1,8) = 2.05$ ,  $p = 0.19$ . **(C)** No change in average VEP amplitude evoked by stimulation of the contralateral (deprived) eye in response to familiar (blue) and novel (red) stimuli in any condition. Inset: Representative VEP waveforms in response to the familiar stimulus in vis stim only (left)  $\alpha\text{E2}$  only (center) and  $\alpha\text{E2}$  + vis stim (right). Stim  $n = 4$ ,  $\alpha\text{E2}$   $n = 5$ ,  $\alpha\text{E2}$  + Stim  $n = 6$ . Males (triangles) vs. females (circles): 2-way ANOVA  $F(1,8) = 1.59$ ,  $p = 0.24$ .

labeling did not co-localize with a nuclear marker in the primary visual cortex or hippocampus, similar to previous reports of high non-nuclear receptor expression in CA1 of adult female rats<sup>23,24</sup>.

In addition to the reduction in circulating sex hormones, the maturation of extracellular matrix (ECM) constrains structural and functional synaptic plasticity in adult circuits<sup>42,64</sup>. A single dose of  $\alpha\text{E2}$  reduced the integrity of the ECM throughout the visual cortex of amblyopic adults, thereby mimicking other interventions that enhance plasticity in adult V1<sup>42,57,63,70</sup>.  $\alpha\text{E2}$  also reduced the expression of PV, a proxy for the excitability of FS INs<sup>13</sup>. However,  $\alpha\text{E2}$  did not induce a global enhancement of plasticity throughout V1.

Acute E2 delivered *in vivo* or *ex vivo* induces robust spinogenesis in the hippocampus of young adult male and female rats<sup>11,25,71,72</sup>, which may be lost with age or following OVX<sup>73</sup>. Brief E2 treatment of hippocampal slices from young males and middle-aged OVX females induces an increase in F-actin, without a change in PSD95 puncta number<sup>14,74</sup>. Similarly, Golgi stains of mouse hippocampus from OVX females (P42) reveal an increase in the number of large, mushroom-type spines following repetitive E2 treatment (1x day/5 days<sup>75</sup>). Following acute delivery of  $\alpha\text{E2}$ , we observed an increase PSD95 puncta size in the adult visual cortex, but no change in the number of PSD95 puncta. Together, this suggests that the estradiols induce the genesis of new excitatory synapses in young adults, and the growth/expansion of pre-existing excitatory synapses in older brains. Importantly, we observed no difference in PSD95 puncta size or number in males versus females, and low variability within the female cohorts suggesting minimal impact of the estrous cycle phase on PSD95 expression in adult rats.

$\alpha\text{E2}$  treatment induced an increase in the size of PSD95 puncta, consistent with the observation that  $\alpha\text{E2}$  treatment alone is sufficient to induce a modest strengthening of excitatory synapses, as reported for E2<sup>76</sup>. Additionally, acute E2 lowers the threshold and increases the magnitude of LTP induced by theta burst stimulation in the hippocampus of OVX rats<sup>68</sup>. However, the absence of an increase in pS831 demonstrates that the increase in the size of excitatory synapses we observe following  $\alpha\text{E2}$  treatment occurs independently of CaMKII/PKC signaling. The observation that estradiol treatment engages a signaling pathway parallel to that engaged by LTP is consistent with reports that the response to acute E2 in hippocampus, including polymerization of actin in dendritic spines and an increase in excitatory synaptic strength, promotes rather than occludes subsequent LTP. An E2-induced increase in excitatory synaptic strength may also underlie reports of increased LTD magnitude<sup>25,76</sup>.

E2 treatment increases the amplitude and frequency of mEPSCs in rat hippocampal CA1 pyramidal neurons in both sexes, indicative of regulation of pre- and postsynaptic function respectively<sup>43</sup>. Importantly, E2-induced changes in mEPSC frequency are limited to synapses with an initially low probability of neurotransmitter release, suggesting that E2 may enhance synaptic function by increasing presynaptic release probability<sup>15</sup>. We observed a similar synapse-specific effect of  $\alpha$ E2 in the adult amblyopic visual cortex, in which the enhancement of activity-dependent plasticity by  $\alpha$ E2 was limited to the pathway serving the non-deprived eye. The observation that the amplitude of the VEP acquired from the deprived eye depresses more rapidly than the non-deprived eye VEP in response to repetitive stimulation suggests that chronic monocular deprivation may increase the probability of neurotransmitter release at deprived-eye synapses<sup>52,53</sup>. The increase in neurotransmitter release probability at synapses serving the deprived eye may occlude the enhancement of plasticity by  $\alpha$ E2 and underlie the selectivity for spared inputs in the amblyopic cortex. The robust expression of ERs in the adult visual cortex and the enhancement of plasticity of synapses in the intact, non-deprived eye pathway by  $\alpha$ E2 suggests that estradiol treatment could be employed to promote the plasticity of spared inputs around a scotoma or a cortical infarct. The selective enhancement of plasticity at synapses with initially low release probability also suggests the possibility that sensitivity to  $\alpha$ E2 reflects the history of synaptic activity, and could be acutely manipulated by activity-dependent changes in the probability of neurotransmitter release.

## Data availability

The datasets generated during the current study are available from the corresponding author on reasonable request.

Received: 20 May 2019; Accepted: 20 November 2019;

Published online: 13 December 2019

## References

- Sherwin, B. B. Estrogen and cognitive functioning in women: lessons we have learned. *Behav. Neurosci.* **126**, 123–7 (2012).
- Rapp, P. R., Morrison, J. H. & Roberts, J. A. Cyclic estrogen replacement improves cognitive function in aged ovariectomized rhesus monkeys. *J. Neurosci.* **23**, 5708–5714 (2003).
- Jacome, F. L. *et al.* Estradiol and ER $\beta$  agonists enhance recognition memory, and DPN, an ER $\beta$  agonist, alters brain monoamines. *Neurobiol. Learn. Mem.* **94**, 488–498 (2010).
- Lu, H., Ma, K., Jin, L., Zhu, H. & Cao, R. 17 $\beta$ -estradiol rescues damages following traumatic brain injury from molecule to behavior in mice. *J. Cell. Physiol.* **233**, 1712–1722 (2018).
- De Macêdo Medeiros, A. *et al.* Estrogen levels modify scopolamine-induced amnesia in gonadally intact rats. *Prog. Neuro-Psychopharmacol. Biol. Psychiatry.* **53**, 99–108 (2014).
- Epperson, C. N., Sammel, M. D. & Freeman, E. W. Menopause effects on verbal memory: findings from a longitudinal community cohort. *J. Clin. Endocrinol. Metab.* **98**, 3829–3838 (2013).
- Hara, Y. *et al.* Estrogen restores multisynaptic boutons in the dorsolateral prefrontal cortex while promoting working memory in aged rhesus monkeys. *J. Neurosci.* **36**, 901–910 (2016).
- Hao, J. *et al.* Estrogen alters spine number and morphology in prefrontal cortex of aged female rhesus monkeys. *J. Neurosci.* **26**, 2571–2578 (2006).
- Zhou, L. *et al.* Aromatase Inhibitors Induce Spine Synapse Loss in the Hippocampus of Ovariectomized Mice. *Endocrinology.* **151**, 1153–1160 (2010).
- Chen, J. R. *et al.* Gonadal hormones modulate the dendritic spine densities of primary cortical pyramidal neurons in adult female rat. *Cereb. Cortex.* **19**, 2719–2727 (2009).
- Gould, E., Woolley, C. S., Frankfurt, M. & McEwen, B. S. Gonadal steroids regulate dendritic spine density in hippocampal pyramidal cells in adulthood. *J. Neurosci.* **10**, 1286–1291 (1990).
- Woolley, C. S. & McEwen, B. S. Roles of estradiol and progesterone in regulation of hippocampal dendritic spine density during the estrous cycle in the rat. *J. Comp. Neurol.* **336**, 293–306 (1993).
- Huang, G. Z. & Woolley, C. S. Estradiol acutely suppresses inhibition in the hippocampus through a sex-specific endocannabinoid and mGluR-dependent mechanism. *Neuron* **74**, 801–808 (2012).
- Kramár, E. A. *et al.* Cytoskeletal changes underlie estrogen's acute effects on synaptic transmission and plasticity. *J. Neurosci.* **29**, 12982–12993 (2009).
- Smejkalova, T. & Woolley, C. S. *J. Neurosci.* **30**, 16137–16148 (2010).
- Adams, M. M. *et al.* Estrogen and aging affect the subcellular distribution of estrogen receptor- $\alpha$  in the hippocampus of female rats. *J. Neurosci.* **22**, 3608–3614 (2002).
- Waters, E. M. *et al.* Estrogen and aging affect the synaptic distribution of estrogen receptor beta-immunoreactivity in the CA1 region of female rat hippocampus. *Brain Res.* **1379**, 86–97 (2011).
- Wilson, M. E. *et al.* Age differentially influences estrogen receptor- $\alpha$  (ER $\alpha$ ) and estrogen receptor- $\beta$  (ER $\beta$ ) gene expression in specific regions of the rat brain. *Mech. Ageing Dev.* **123**, 593–601 (2002).
- Lai, Y. J., Yu, D., Zhang, J. H. & Chen, G. J. Cooperation of genomic and rapid nongenomic actions of estrogens in synaptic plasticity. *Mol. Neurobiol.* **54**, 4113–4126 (2017).
- Srivastava, D. P. D. *et al.* Rapid estrogen signaling in the brain: implications for the fine-tuning of neuronal circuitry. *J. Neurosci.* **31**, 16056–16063 (2011).
- Babayán, A. H. & Kramár, E. A. Rapid effects of oestrogen on synaptic plasticity: interactions with actin and its signalling proteins. *J. Neuroendocrinol.* **25**, 1163–1172 (2013).
- Fan, L. *et al.* Estradiol-induced object memory consolidation in middle-aged female mice requires dorsal hippocampal extracellular signal-regulated kinase and phosphatidylinositol 3-kinase activation. *J. Neurosci.* **30**, 4390–4400 (2010).
- Milner, T. A. *et al.* Ultrastructural localization of estrogen receptor  $\beta$  immunoreactivity in the rat hippocampal formation. *J. Comp. Neurol.* **491**, 81–95 (2005).
- Milner, T. A. *et al.* Ultrastructural evidence that hippocampal alpha estrogen receptors are located at extranuclear sites. *J. Comp. Neurol.* **429**, 355–371 (2001).
- Mukai, H. *et al.* Rapid modulation of long-term depression and spinogenesis via synaptic estrogen receptors in hippocampal principal neurons. *J. Neurochem.* **100**, 950–967 (2007).
- Sellers, K. J. *et al.* Rapid modulation of synaptogenesis and spinogenesis by 17 $\beta$ -estradiol in primary cortical neurons. *Front. Cell. Neurosci.* **9**, 1–11 (2015).

27. Hart, S. A., Snyder, M. A., Smejkalova, T. & Woolley, C. S. Estrogen mobilizes a subset of estrogen receptor- $\alpha$ -immunoreactive vesicles in inhibitory presynaptic boutons in hippocampal CA1. *J. Neurosci.* **27**, 2102–2111 (2007).
28. Jeong, J. K., Tremere, L. A., Burrows, K., Majewska, A. K. & Pinaud, R. The mouse primary visual cortex is a site of production and sensitivity to estrogens. *PLoS One.* **6**, 1–12 (2011).
29. Mitra, S. W. *et al.* Immunolocalization of estrogen receptor  $\beta$  in the mouse brain: comparison with estrogen receptor  $\alpha$ . *Endocrinology.* **144**, 2055–2067 (2003).
30. Shughrue, P. J. & Merchenthaler, I. Distribution of estrogen receptor  $\beta$  immunoreactivity in the rat central nervous system. *J. Comp. Neurol.* **436**, 64–81 (2001).
31. Simerly, R. B., Chang, C., Muramatsu, M. & Swanson, L. W. Distribution of androgen and estrogen receptor mRNA-containing cells in the rat brain: an *in situ* hybridization study. *J. Comp. Neurol.* **294**, 76–95 (1990).
32. Yokosuka, M., Okamura, H. & Hayashi, S. Transient expression of estrogen receptor-immunoreactivity (ER-IR) in the layer V of the developing rat cerebral cortex. *Dev. Brain Res.* **84**, 99–108 (1995).
33. He, H.-Y., Ray, B., Dennis, K. & Quinlan, E. M. Experience-dependent recovery of vision following chronic deprivation amblyopia. *Nat. Neurosci.* **10**, 1134–1136 (2007).
34. Mitchell, D. E. & MacKinnon, S. The present and potential impact of research on animal models for clinical treatment of stimulus deprivation amblyopia. *Clin. Exp. Optom.* **85**, 5–18 (2002).
35. Montey, K. L. & Quinlan, E. M. Recovery from chronic monocular deprivation following reactivation of thalamocortical plasticity by dark exposure. *Nat. Commun.* **2**, 317–318 (2011).
36. MacLusky, N. J., Luine, V. N., Hajszan, T. & Leranath, C. The 17 $\alpha$  and 17 $\beta$  isomers of estradiol both induce rapid spine synapse formation in the CA1 hippocampal subfield of ovariectomized female rats. *Endocrinology.* **146**, 287–293 (2005).
37. Toran-Allerand, C. D., Tinnikov, A. A., Singh, R. J. & Nethrapalli, I. S. 17 $\alpha$ -Estradiol: a brain-active estrogen? *Endocrinology.* **146**, 3843–3850 (2005).
38. Rumi, M. A. K. *et al.* Defining the role of estrogen receptor  $\beta$  in the regulation of female fertility. *Endocrinology* **158**, 2330–2343 (2017).
39. Kuiper, G. G., Enmark, E., Peltö-Huikko, M., Nilsson, S. & Gustafsson, J. A. Cloning of a novel receptor expressed in rat prostate and ovary. *Proc. Natl. Acad. Sci. USA* **93**, 5925–30 (1996).
40. Davidson, N. E., Gelmann, E. P., Lippman, M. E. & Dickson, R. B. Epidermal growth factor receptor gene expression in estrogen receptor-positive and negative human breast cancer cell lines. *Mol. Endocrinol.* **1**, 216–223 (1987).
41. Chavez, K. J., Garimella, S. V. & Lipkowitz, S. Triple negative breast cancer cell lines: one tool in the search for better treatment of triple negative breast cancer. *Breast Dis.* **32**, 35–48 (2010).
42. Murase, S., Lantz, C. L. & Quinlan, E. M. Light reintroduction after dark exposure reactivates plasticity in adults via perisynaptic activation of MMP-9. *ELife.* **6**, 1–23 (2017).
43. Oberlander, J. G. & Woolley, C. S. 17 $\beta$ -Estradiol acutely potentiates glutamatergic synaptic transmission in the hippocampus through distinct mechanisms in males and females. *J. Neurosci.* **36**, 2677–2690 (2016).
44. Coleman, J. E., Law, K. & Bear, M. F. Anatomical origins of ocular dominance in mouse primary visual cortex. *Neuroscience.* **161**(2), 561–571 (2009).
45. Khibnik, L. A., Cho, K. K. & Bear, M. F. Relative contribution of feedforward excitatory connections to expression of ocular dominance plasticity in layer 4 of visual cortex. *Neuron.* **66**, 493–500 (2010).
46. Frenkel, M. Y. & Bear, M. F. How monocular deprivation shifts ocular dominance in visual cortex of young mice. *Neuron* **44**, 917–923 (2004).
47. Tagawa, Y., Kanold, P. O., Majdan, M. & Shatz, C. J. Multiple periods of functional ocular dominance plasticity in mouse visual cortex. *Nat. Neurosci.* **8**, 380–388 (2005).
48. Derkach, V., Barria, A. & Soderling, T. R. Ca<sup>2+</sup>/calmodulin-kinase II enhances channel conductance of  $\alpha$ -amino-3-hydroxy-5-methyl-4-isoxazolepropionate type glutamate receptors. *Proc. Natl. Acad. Sci. USA* **96**, 3269–3274 (1999).
49. Hu, H. *et al.* Emotion enhances learning via norepinephrine regulation of AMPA-receptor trafficking. *Cell.* **131**, 160–73 (2007).
50. Whitlock, J. R., Heynen, A. J., Shuler, M. G. & Bear, M. F. Learning induces long-term potentiation in the hippocampus. *Science.* **313**, 1093–1097 (2006).
51. Eaton, N. C., Sheehan, H. M. & Quinlan, E. M. Optimization of visual training for full recovery from severe amblyopia in adults. *Learn. Memory.* **23**, 99–103 (2016).
52. Krahe, T. E. & Guido, W. Homeostatic plasticity in the visual thalamus by monocular deprivation. *J. Neurosci.* **31**, 6842–6849 (2011).
53. Yashiro, K., Corlew, R. & Philpot, B. D. Visual deprivation modifies both presynaptic glutamate release and the composition of perisynaptic/extrasynaptic NMDA receptors in adult visual cortex. *J. Neurosci.* **25**, 11684–11692 (2005).
54. Zancan, M., Dall'Oglio, A., Quagliotto, E. & Rasia-Filho, A. A. Castration alters the number and structure of dendritic spines in the male posterodorsal medial amygdala. *Eur. J. Neurosci.* **45**, 572–580 (2017).
55. Duffy, K. R. & Mitchell, D. E. Darkness alters maturation of visual cortex and promotes fast recovery from monocular deprivation. *Curr. Biol.* **23**, 382–386 (2013).
56. Gu, Y. *et al.* Neuregulin-dependent regulation of fast-spiking interneuron excitability controls the timing of the critical period. *J. Neurosci.* **36**, 10285–10295 (2016).
57. Pizzorusso, T. *et al.* Structural and functional recovery from early monocular deprivation in adult rats. *Proc. Natl. Acad. Sci. USA* **103**, 8517–8522 (2006).
58. Tognini, P. *et al.* Environmental enrichment promotes plasticity and visual acuity recovery in adult monocular amblyopic rats. *PLoS One.* **7**, e34815 (2012).
59. Donato, F., Rompani, S. B. & Caroni, P. Parvalbumin-expressing basket-cell network plasticity induced by experience regulates adult learning. *Nature.* **504**, 272 (2013).
60. Fugger, H. N., Kumar, A., Lubahn, D. B., Korach, K. S. & Foster, T. C. Examination of estradiol effects on the rapid estradiol mediated increase in hippocampal synaptic transmission in estrogen receptor  $\alpha$  knockout mice. *Neurosci. Lett.* **309**, 207–209 (2001).
61. Kumar, A., Bean, L. A., Rani, A., Jackson, T. & Foster, T. C. Contribution of estrogen receptor subtypes, ER $\alpha$ , ER $\beta$ , and GPER1 in rapid estradiol-mediated enhancement of hippocampal synaptic transmission in mice. *Hippocampus.* **25**, 1556–1566 (2015).
62. Kumar, A. & Foster, T. C. 17 $\beta$ -Estradiol Benzoate Decreases the AHP Amplitude in CA1 Pyramidal Neurons. *J. Neurophysiol.* **88**, 621–626 (2002).
63. Carulli, D. *et al.* Animals lacking link protein have attenuated perineuronal nets and persistent plasticity. *Brain.* **133**, 2331–2347 (2010).
64. Pizzorusso, T. *et al.* Reactivation of ocular dominance plasticity in the adult visual cortex. *Science.* **298**, 1248–1251 (2002).
65. Frenkel, M. Y. *et al.* Instructive effect of visual experience in mouse visual cortex. *Neuron.* **51**, 339–349 (2006).
66. Eavri, R. *et al.* Interneuron simplification and loss of structural plasticity as markers of aging-related functional decline. *J. Neurosci.* **38**, 8421–8432 (2018).
67. Montey, K. L., Eaton, N. C. & Quinlan, E. M. Repetitive visual stimulation enhances recovery from severe amblyopia. *Learn. Memory.* **20**, 311–317 (2013).
68. Córdoba Montoya, D. A. & Carrer, H. F. Estrogen facilitates induction of long term potentiation in the hippocampus of awake rats. *Brain Res.* **778**, 430–438 (1997).

69. Hojo, Y. *et al.* Estradiol rapidly modulates spinogenesis in hippocampal dentate gyrus: involvement of kinase networks. *Horm. Behav.* **74**, 149–156 (2015).
70. Sale, A. *et al.* Environmental enrichment in adulthood promotes amblyopia recovery through a reduction of intracortical inhibition. *Nat. Neurosci.* **10**, 679–681 (2007).
71. Cooke, S. F. & Bear, M. F. Stimulus-selective response plasticity in the visual cortex: an assay for the assessment of pathophysiology and treatment of cognitive impairment associated with psychiatric disorders. *Biol. Psychiatry.* **71**, 487–95 (2012).
72. Phan, A. *et al.* Rapid increases in immature synapses parallel estrogen-induced hippocampal learning enhancements. *Proc. Natl. Acad. Sci. USA* **112**, 16018–16023 (2015).
73. Adams, M. M., Shah, R. A., Janssen, W. G. & Morrison, J. H. Different modes of hippocampal plasticity in response to estrogen in young and aged female rats. *Proc. Natl. Acad. Sci. USA* **98**, 8071–8076 (2001).
74. Wang, W. *et al.* Estrogen's effects on excitatory synaptic transmission entail integrin and TrkB transactivation and depend upon  $\beta 1$ -integrin function. *Neuropsychopharmacol.* **41**, 2723–2732 (2016).
75. Li, C. *et al.* Estrogen alters hippocampal dendritic spine shape and enhances synaptic protein immunoreactivity and spatial memory in female mice. *Proc. Natl. Acad. Sci. USA* **101**, 2185–2190 (2004).
76. Kramár, E. A., Babayan, A. H., Gall, C. M. & Lynch, G. Estrogen promotes learning-related plasticity by modifying the synaptic cytoskeleton. *Neuroscience.* **239**, 3–16 (2013).

## Acknowledgements

This work was supported by NIH R01EY016431 (to E.M.Q.), and an ARCS-MWC Foundation Fellowship, a UM NACS Hodos Dissertation Completion Fellowship and a Cosmos Club Foundation Scholars Fellowship (to D.C.S.).

## Author contributions

D.C.S. performed the experiments in Figures 1, 2A, 2B, 3, 4, and 5. C.L.L. performed the experiments in Figures 2C and 6. M.A.K.R. provided the ER $\beta^{-/-}$  rats and contributed to data interpretation. D.C.S., C.L.L. and E.M.Q. designed the experiments and wrote the manuscript.

## Competing interests

Deepali C. Sengupta declares she has no competing interests. Crystal L. Lantz declares she has no competing interests. M.A. Karim Rumi declares he has no competing interests. Elizabeth M. Quinlan declares she has no competing interests.

## Additional information

**Correspondence** and requests for materials should be addressed to E.M.Q.

**Reprints and permissions information** is available at [www.nature.com/reprints](http://www.nature.com/reprints).

**Publisher's note** Springer Nature remains neutral with regard to jurisdictional claims in published maps and institutional affiliations.



**Open Access** This article is licensed under a Creative Commons Attribution 4.0 International License, which permits use, sharing, adaptation, distribution and reproduction in any medium or format, as long as you give appropriate credit to the original author(s) and the source, provide a link to the Creative Commons license, and indicate if changes were made. The images or other third party material in this article are included in the article's Creative Commons license, unless indicated otherwise in a credit line to the material. If material is not included in the article's Creative Commons license and your intended use is not permitted by statutory regulation or exceeds the permitted use, you will need to obtain permission directly from the copyright holder. To view a copy of this license, visit <http://creativecommons.org/licenses/by/4.0/>.

© The Author(s) 2019